ORIGINAL RESEARCH

Process optimization of biodiesel production catalyzed by CaO nanocatalyst using response surface methodology

Priyanka Bharti[1] · Bhaskar Singh[1] · R. K. Dey[2]

Abstract

Uses of nanocatalysts have become more useful in optimizing catalytic reactions. They are known to enhance the rate of reaction by offering a greater number of active sites by possessing a high surface-to-volume ratio. In the present work, calcium oxide nanocatalysts were synthesized through the sol–gel method. The particle size of the nanocatalyst prepared ranged up to 8 nm. Soybean oil was used as the raw material for the synthesis of biodiesel. The synthesized nano-CaO was characterized through scanning electron microscopy (SEM), transmission electron microscopy (TEM), X-ray diffraction (XRD), Fourier transform infrared spectroscopy (FTIR) and BET (Brunauer–Emmett–Teller). Average BET surface area analysis of the nanocatalyst was calculated to be 67.781 m^2/g and pore diameter was 3.302 nm. Nano-CaO catalyst was used to synthesize biodiesel and optimize the reaction variables through optimization processes to achieve a high yield of biodiesel. The reaction variables that were optimized were catalyst amount, oil to methanol molar ratio and reaction temperature. Upon optimization, the conversion of biodiesel was found to be 97.61%. The optimized value of the reaction variables was: catalyst amount of 3.675 wt% with respect to oil, molar ratio (alcohol to oil) of 11:1, and reaction temperature of 60 °C for 2 h.

Graphic abstract
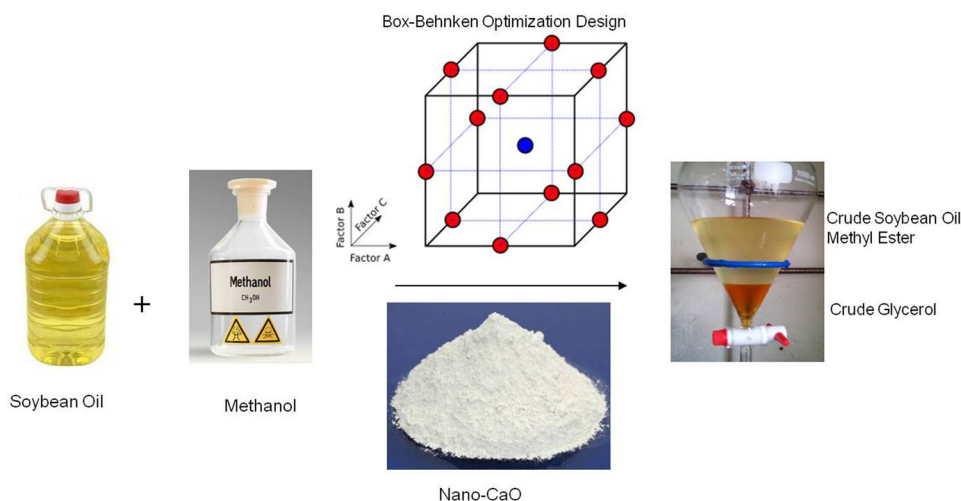
Keywords Biodiesel · Calcium oxide (CaO) · Nanocatalyst · Response surface methodology

✉ Bhaskar Singh
   bhaskar.singh@cuj.ac.in

✉ R. K. Dey
   rkdey@rediffmail.com

Extended author information available on the last page of the article

Introduction

Renewable energy has attracted the interest of researchers worldwide owing to diminishing fossil fuel reserves and environmental concerns [1]. Biodiesel composed of fatty

🖂 Springer

acid alkyl esters is one of the prominent renewable fuels that is considered clean, non-toxic, sulfur and aromatic free when compared with petroleum-based diesel fuel [2]. Biodiesel can be produced from a variety of vegetable oil, algal oil, or animal fat in combination with an alcohol (e.g., methanol) in the presence of a catalyst. A by-product, glycerol, is also obtained in the process. Currently, plant oil is the conventional feedstock currently used in the production of biodiesel owing to its availability worldwide. The catalyst used in the reaction may be either homogeneous or heterogeneous. Homogeneous catalysts commonly used for the reaction are sodium hydroxide and potassium hydroxide owing to their low cost [3]. Several heterogeneous catalysts have also been explored in the synthesis of biodiesel by researchers. Heterogeneous catalysts are advantageous over homogeneous catalysts because they can be reused. Calcium oxide-based heterogeneous catalysts have been commonly used in the synthesis processes for biodiesel production because of their high catalytic activity, low cost, non-toxicity, and easy availability [4–6]. CaO is also environmentally friendly. CaO-based catalysts can be extracted from various compounds in which calcium is present as oxides, hydroxides, carbonates, and alkoxides. The catalytic activity, basicity and surface area of CaO have been reported to be enhanced by calcination, hydration, and dehydration process. A high fatty acid methyl ester (FAME) yield of 95% has been reported at 5 wt% of catalyst loading, methanol to oil molar ratio of 12:1 for 5 h at room temperature (30 ± 2 °C) [7]. A recent study done by Todorovic et al. [8] reported optimization of reaction variables in the production of biodiesel using CaO as a catalyst and crude biodiesel as a co-solvent. Optimum reaction conditions of methanol to oil molar ratio 7.1:1, catalyst concentration of 0.74 mol/L, and reaction temperature of 52 °C were reported to yield a high FAME conversion of 99.8%. The catalyst was reused for four times under the reaction conditions of methanol to oil molar ratio, 6:1; catalyst concentration, 0.642 mol/L; reaction temperature, 50 °C; and reaction time, 1.5 h, which gave a FAME conversion of 97.7% in 5 h at the second cycle [8].

Degirmenbasi et al. [9] reported that higher conversion rate could be achieved if CaO nanoparticles possessing a high surface to volume ratio are used. The nano-CaO with high basicity was reported to functionalize with K_2CO_3. The use of nanocatalyst impregnated with K_2CO_3 was reported to enhance the rate of transesterification reaction that was attained at a moderate temperature of 65 °C. The reaction order was reported to be 0.98. A low value of activation energy of 25.34 ± 2.48 kJ/mol was an indication of the reaction being mass controlled. $CuFe_2O_4$-doped CaO nanocatalyst prepared by chemical precipitation method has been reported by Seffati et al. [10] to produce biodiesel with a high yield of 94.52% at moderate reaction conditions of methanol to oil molar ratio of 15:1, reaction time of 4 h,

and catalyst content of 3% at 70 °C. The advantage offered by the nanocatalyst reported is high porosity that offers a greater number of active sites. Incorporating $CuFe_2O_4$ with CaO magnetic properties was helpful in its easy separation from the product. Hu et al. [11] have reported porous structure of $KF/CaO-Fe_3O_4$ used as nano-magnetic catalyst for synthesis of biodiesel. The catalyst was reported to possess particle diameter of about 50 nm. The BET surface area was 20.08 m^2/g compared to only 4.6 m^2/g for CaO. Salimi and Hosseini [12] reported that using magnetic nanocatalyst could be helpful in its easy separation from the reaction products by applying magnetic field. The $ZnO/BiFeO_3$ nanocatalyst showed a high catalytic activity with a biodiesel yield of 95.43 and 95.02% in first and second run, respectively.

Badnore et al. [13] reported that nano-crystalline CaO has a specific surface area that is 1.54 times higher than commercial calcium oxide. Owing to high surface area of 97.63 m^2/g, the nano-sized catalyst showed 18.81% higher conversion than the commercially available CaO catalyst (with a surface area of 74.64 m^2/g) at similar operating conditions. The high surface area has been attributed to the small crystallite and particle size of the catalyst. A large surface area increases the reaction rate. The conversion of soybean oil to biodiesel was obtained at moderate reaction conditions of methanol to oil molar ratio of 6:1 and catalyst content of 4% at 60 °C for 80 min. With a small diameter and high specific surface area of nano-CaO, Hebbar et al. [14] have reported a high yield (96.2%) of biodiesel at moderate reaction conditions of 10.37:1 molar ratio of methanol to oil, 1.5 wt % catalyst amount, at 65 °C with a mixing speed of 600 rpm. The activation energy was 35.99 kJ/mol. Hsiao et al. [15] reported that nano-CaO was highly effective as compared to larger sized CaO for production of biodiesel using microwave irradiation. A high conversion of 71.6% was reported with nano-CaO compared to only 2.3% with larger-sized CaO when the same amount of catalyst (1 wt %) was used with 6:1 methanol to oil molar ratio at 60 °C for 30 min.

Banković–Ilić et al. [16] gave an excellent review of the application of nano-sized CaO in the synthesis of biodiesel. It has been reported that nano-CaO could be used in neat, doped (with other compounds using CaO as carrier) and loaded form (immobilization of CaO onto a different carrier). The advantages offered by nano-CaO are its reusability and restraint to leaching. Neat nano-CaO can be reused for three and eight cycles, respectively, without any significant decline in catalytic activity. Nano-CaO consists of numerous crystallites with well-defined edges. Upon reuse of the catalyst, these well-defined edges are converted to aggregates of polycrystals with edges that are less well defined. The kinetics of reaction while using nano-CaO has been reported to follow a pseudo-first-order kinetic model. The activation

energy using neat-CaO is usually high but is lowered when loaded or doped with another compound.

Apart from synthesis of biodiesel, extensive work has been reported by researchers worldwide in the use of nanoparticles, i.e., treatment of harmful organic compounds through adsorption, etc. [17–37]. It is expected that having a small particle pore size and a high specific surface area using nano-CaO will be effective in reducing energy consumption by lowering the reaction time and temperature.

This study investigates using nano-CaO to achieve a higher conversion of oil to biodiesel in a shorter reaction time (2 h). Soybean oil will be catalyzed by synthesized nano-CaO to produce biodiesel. The effect of various reaction conditions on the conversion of biodiesel will be done using 15 random reactions. The influence of different reaction parameters (molar ratio, catalyst concentration, and reaction temperature) will be evaluated using Response Surface Methodology (RSM) through the Box–Behnken model.

Materials and methods

Materials

Edible grade refined soybean oil (Brand: Fortune) was purchased from a local market. Methanol ($\geq 99\%$), calcium nitrate tetrahydrate ($\geq 98\%$), and sodium hydroxide pellets ($\geq 97\%$) were purchased from Merck India, while ethylene glycol (98%) was purchased from Thermo Fisher.

Catalyst synthesis

Calcium oxide nanocatalyst was synthesized through sol–gel method using the method described by Tahvildari et al. [38]. A known amount of Calcium nitrate tetrahydrate was dissolved in distilled water to which 25 mL of ethylene glycol was added under continuous stirring. A small amount of sodium hydroxide pellets was dissolved in distilled water and added to the latter solution drop-by-drop. The mixture was stirred for 2 h. The gel was initially heated at 105 °C for 2 h for the vaporization of the aqueous layer and was later kept still for 1 h. The gel was filtered using Whatman filter paper (Grade 3) and washed four times with distilled water to reduce the basicity of the medium. The washed gel was dried in a hot air oven at 105 °C for 4 h. The dried gel was ground to a fine powder using a mortar pestle. The dried powder calcium oxide nanocatalyst was calcined at 850 °C for 1 h and stored in a desiccator.

Catalyst characterization

The functional groups present on the catalyst surface were identified with the help of Fourier Transform Infrared Spectroscopy (FTIR) on IR-Prestige 21(Shimadzu Corpn, Japan) in the IR range of 500–4000 cm^{-1}. The X-ray diffractogram (XRD) pattern of nanocatalyst was recorded on a Proto A-XRD automated diffractometer between 10° and 80° at a ramping rate of 10° min^{-1}. The morphological structure of nanocatalyst was studied through Scanning Electron Microscopy (SEM) on LEO 435 VP, while the particle dimensions of nanocatalyst were obtained through transmission electron microscopy (TEM) on FEI Technai G^2 20 S-Twin. Brunauer–Emmett–Teller (BET) surface area characterization of CaO nanocatalyst was performed on Quantachrome/AUTOSORB-1.

Transesterification of soybean oil

The transesterification reaction was performed in a conical flask equipped with a reflux condenser on a temperature-controlled magnetic stirrer with hot plate. The soybean oil was preheated at 105 °C to eliminate the influence of moisture. Methanol and catalyst (nano-CaO) were initially mixed in a conical flask at 65 °C under constant stirring for 15 min. The soybean oil at the desired reaction temperature was later added to the methanolic solution of the catalyst. The above mixture was allowed to react for 2 h. Afterward, the contents of the flask were transferred to a separating funnel for the separation of the biodiesel and glycerol layers based on their density and solubility differences.

Glycerol was decanted from the separatory funnel. The crude biodiesel was heated to remove the excess methanol present. The conversion of biodiesel was estimated by ^{1}H nuclear magnetic resonance (NMR) spectroscopy as per the relationship provided in Eq. 1 [39]:

$$C\,(\%) = 100 \times (2A_{ME}/3A_{CH_2}), \tag{1}$$

where C is the content of fatty acid methyl ester, A_{ME} is the integration value of methoxy protons (appears at 3.6 ppm) and A_{CH2} is the integration value of methylene protons (appears at 2.3 ppm)

Design of experiments

RSM is widely used in the optimization of the reaction conditions for biodiesel production [40]. The optimization of reaction variables was achieved with the help of RSM based Box–Behnken Design using the statistical package of Minitab-18. The independent variables, their designated symbols, and analyzed levels are shown in Table 1. All reactions were conducted for 2 h.

The experimental design consisted of a total of 15 experiments comprising 12 factorial point experiments with 3 replicates at the center point (Table 2). To analyze the effect of individual factors and their analyzed levels, the experimental

Table 1 Independent variables for the transesterification of soybean oil using Box–Behnken model

Variables	Symbols	Levels		
		Low value	Mid value	High value
Catalyst concentration (wt.%)	A	2.850	3.675	4.500
Methanol/oil molar ratio	B	10	11	12
Reaction temperature (°C)	C	55	60	65

Table 2 Experiment design of various reaction parameters, their conversion percentage and predicted values

Base runs	A: Catalyst amount (%)	B: Methanol/oil ratio	C: Reaction temperature (°C)	Biodiesel conversion (%)	Predicted value (%)
1	3.675	12	65	97.44	94.40
2	3.675	11	60	97.61	90.64
3	4.500	12	60	96.42	97.82
4	2.850	12	60	89.40	87.00
5	4.500	11	55	94.89	89.45
6	3.675	12	55	59.44	63.47
7	4.500	11	65	78.04	79.67
8	4.500	10	60	96.22	98.61
9	2.850	11	65	84.91	90.34
10	2.850	11	55	64.95	63.31
11	3.675	10	65	80.00	75.96
12	3.675	11	60	97.61	90.64
13	3.675	10	55	86.60	89.64
14	2.850	10	60	95.35	93.94
15	3.675	11	60	96.61	90.64

response was fitted to a second-order polynomial model (Eq. 2):

$$Y = \beta_o + \sum_{i=1}^{3} \beta_i x_i + \sum_{i=1}^{3} \beta_{ii} x_i^2 + \sum_{i=1}^{2} \sum_{j=i+1}^{3} \beta_{ij} x_{ij} + \varepsilon, \qquad (2)$$

where Y is the conversion of the soybean oil to biodiesel (in percentage); βo, β_i, β_{ii} and β_{ij} represent the regression coefficient for the intercept, linear term, quadratic term, and the interactive term, respectively; x_i, and xj are the independent variables; and ε is the model error. The statistical analysis of the model was performed through ANOVA and fit statistics [41]. The effect of the independent variables was assessed with the help of contour and response surface plots.

# Results and discussion

Characterization of the catalyst

The FTIR spectra of CaO are shown in Fig. 1. The Ca–O vibrations appeared at around 500 cm^{-1}. The absorption at 1438 cm^{-1} marks the presence of carbonate species while the vibrations of hydroxide appear at 3641 cm^{-1}. Because the hygroscopic nature of Ca–O is well recognized, the appearance of Ca(OH)$_2$ spectra is justified; the presence of CaCO$_3$ is due to the absorption of atmospheric CO$_2$. The characteristic signals at 500 cm^{-1} suggested the synthesis of Ca–O. Hebbar et al. [14] have reported a strong peak at wavenumber 703.23 cm^{-1}, which was attributed to stretching vibrations of Ca–O bonds. The broad peaks at 1790 and 3423 cm^{-1} were due to the presence of ⁻OH stretching and deformation, respectively. This could be attributed to absorption of water by the catalyst.

XRD pattern of synthesized nano-CaO showed peaks characteristic for cubic CaO (Fig. 2). The powder form of catalyst was scanned in the range of 10°–90°. The diffraction peaks observed were at $2\theta = 31°$, 34°, 37°, and 54° that exhibited a high degree of similarity with the standard ICDD (The International Centre for Diffraction Data) file for CaO (JCPDS 37-1497). The XRD and FTIR spectra confirmed high purity and crystallinity of CaO. The average crystallite size of the CaO nanocatalyst was determined by the Debye–Scherrer equation (Eq. 3) and was estimated to be ~ 8 nm with cubic structure.

$$D = K \times \text{Wavelength (in nanometers)}/\text{FWHM} \cos \theta, \qquad (3)$$

Fig. 1 FTIR spectrum of synthesized calcium oxide nanocatalyst
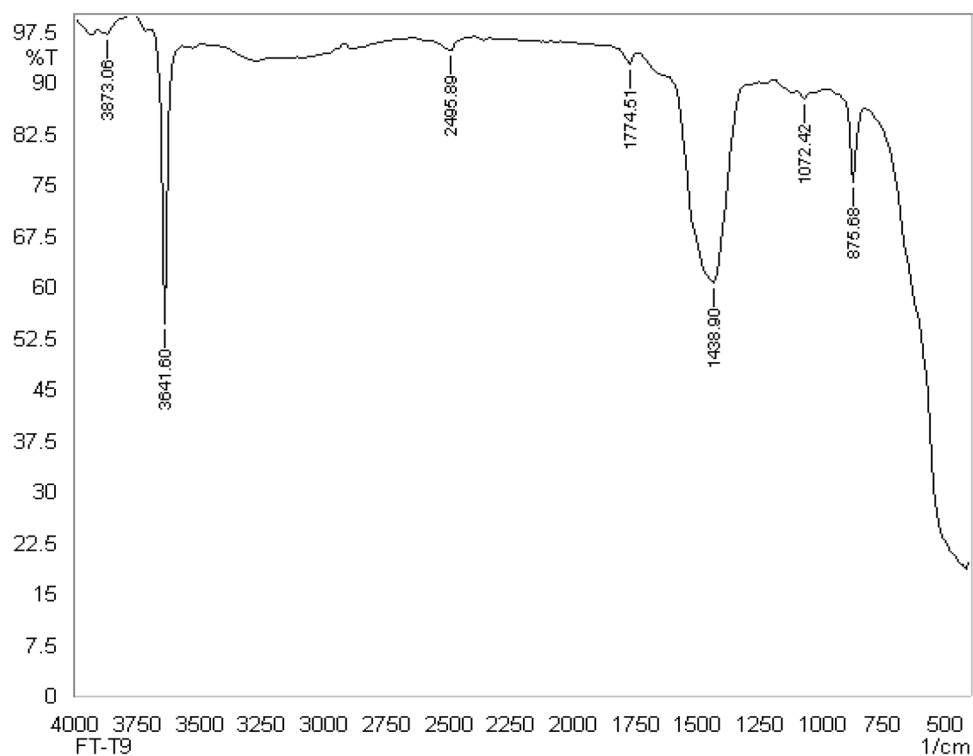
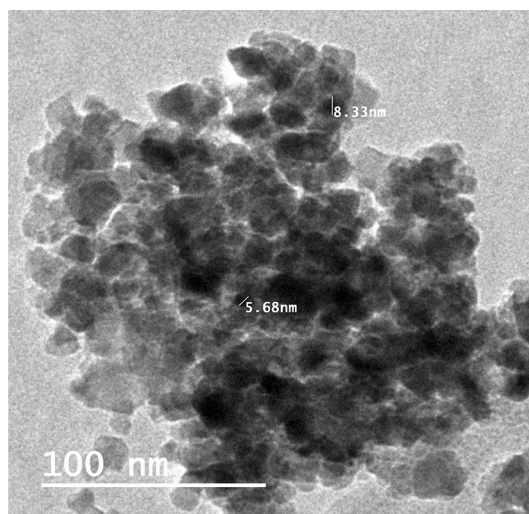**Fig. 2** XRD pattern of synthesized calcium oxide nanocatalyst
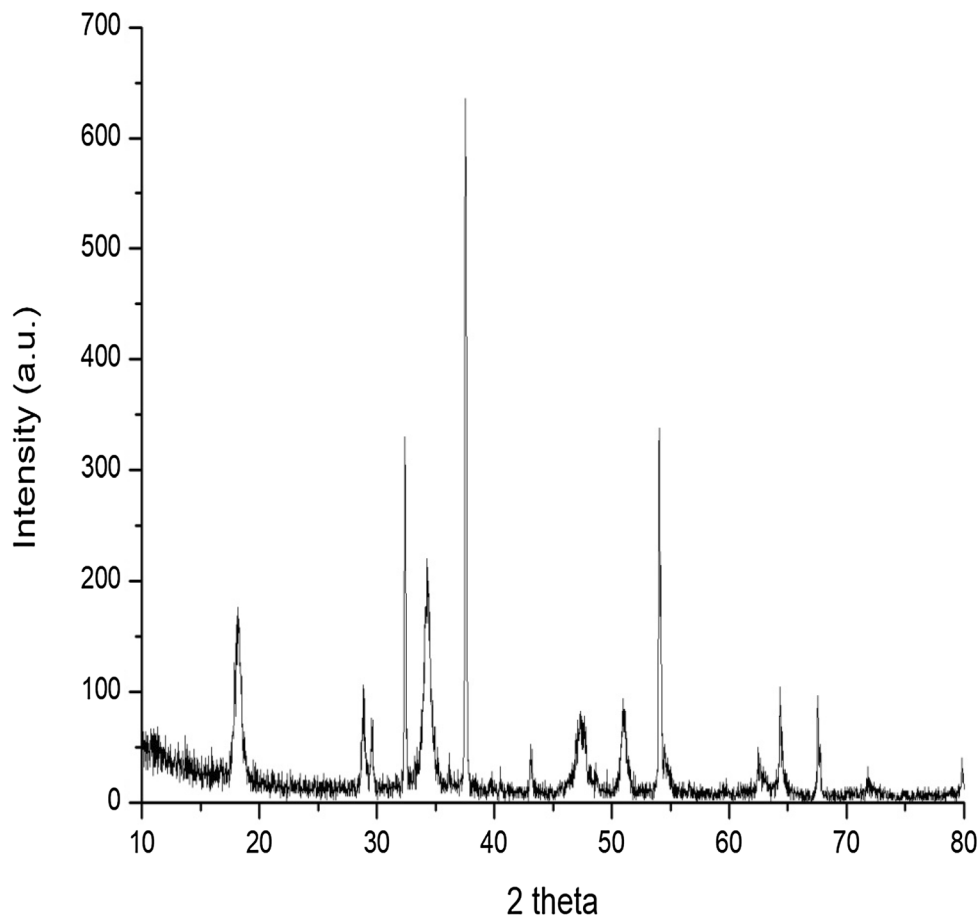
where K is the crystalline shape factor (0.9), FWHM is the full width at half maximum, and θ is the Bragg's angle.

A similar XRD high intense peak at $2\theta = 37.42°$ was reported by Badnore et al. [13].

The morphological nature of grain observed shows spherical shape of particles in the form of agglomerates (Fig. 3). The particles are densely agglomerated with each other with a regular shape. The surface micrograph of synthesized nanocatalysts appeared as rough surface and fracture. The particles were observed to be uneven. Image shows high porosity and material is amorphous in nature and structure. There is a nodule formation that indicates the binding of CaO–CaO. A neat blocky structure (from mixed CaO and MgO) is reported to offer better water resistance to the catalyst as compared to pure structure offered by neat CaO [42]. A regular and ordered shape offers an advantage of having a better interconnected regular pore distribution system [43].

Transmission electron microscopy images are useful in identifying the mesoporous structure of the compound. A hexagonal array of mesopores in this study indicated a highly ordered mesoporous structure [44]. The TEM image of synthesized nanoparticles is shown in Fig. 4. The particles observed were spherical in nature. The synthesized nanocatalyst showed a uniform particle size with the average particles size ranging from 5.68 to 8.33 nm. Some scattered particles were 100 nm diameter. The particle size observed by TEM is in good agreement with the average crystallite size as estimated by XRD. The bonding of


Fig. 4 Transmission electron micrograph of synthesized calcium oxide nanocatalyst

CaO nano-particles results in the formation of aggregates as explained by the TEM micrograph. The small size and aggregations of the particles created a high specific surface area to the nano-CaO.

The specific surface area of the synthesized CaO nanocatalyst was 67.781 $m^2 g^{-1}$ and the average pore diameter was 3.302 nm. The surface area of CaO has been reported to be 13 $m^2 g^{-1}$, which is significantly lower than that

Fig. 3 Scanning electron micrograph of synthesized calcium oxide nanocatalyst
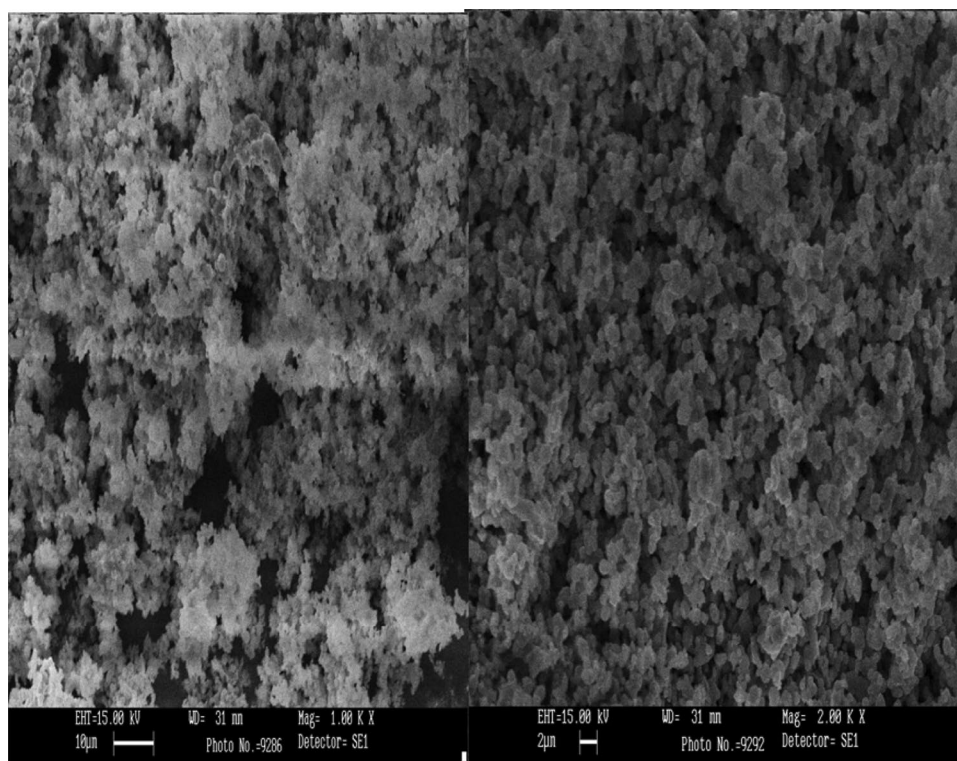
of nano-CaO [45]. A high surface area of 97.63 m^2 g^{-1} for nano-CaO and comparatively lower surface area of 74.64 m^2 g^{-1} for commercial CaO has been reported by Badnore et al. [13]. Pandit and Fulekar [46] reported a specific surface area of 15.73 m^2 g^{-1} and average pore diameter of 3 nm with nano-CaO. A high specific surface area and smaller pore diameter impart mesopores in the catalyst that make the catalyst suitable for reaction through adsorption. A high surface area is characteristic of high porosity and high functionality of the compound. With high surface area, a greater number of active sites are available [47]. Awual et al. [48] reported that spherical nano-sized cavities possess a large surface area as compared to other particles. Nanoparticles have an improved surface morphology in the form of surface area, pore size, and pore volume as compared to larger particles. A large surface area and pore size have better adsorption capability for trace metal ions [49]. A similar advantage could also be attributed for conversion of oil to FAME through adsorption by nanocatalyst.
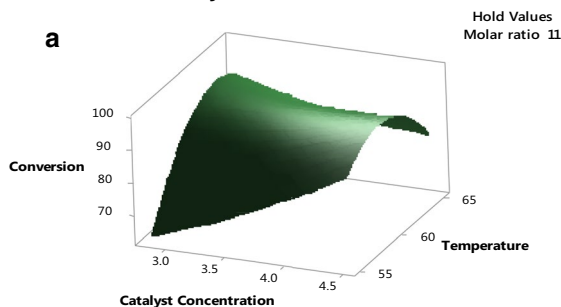
Optimization of reaction variable for transesterification

RSM was utilized to study the effect of different reaction variables on the conversion of oil to FAME. The Box–Behnken design is an effective tool of response surface methodology that can be used to optimize a response that is dependent on multiple factors. At a low catalyst concentration (2.850 wt.%), molar ratio (11:1; methanol to oil), and reaction temperature (55 °C), the conversion was low (64.95%). With an increase in temperature (65 °C), the conversion reached 84.91%. The lowest conversion was recorded for run number 6, which involved a catalyst loading of 3.675%, molar ratio of 12:1 (methanol to oil), and reaction temperature of 55 °C. The highest conversion of 97.61% was attained at a catalyst loading, molar ratio (methanol to oil), and reaction temperature of 3.675%, 11:1, and 60 °C, respectively (run numbers 2 and 12). At the highest catalyst concentration (4.500 wt.%), the conversion was slightly lower. A catalyst loading of 3.675 wt.% is the most efficient concentration for the reaction as it led to a high degree of conversion irrespective of the settings for the remainder of the factors. The response surface and contour plots were generated while holding one factor constant at the center point while the other two were varied over their entire range of operation.
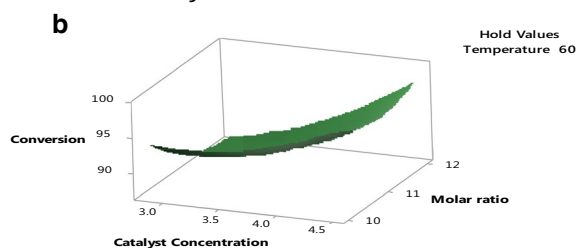
The response surface plots for conversion were plotted against catalyst concentration and reaction temperature (Fig. 5a); catalyst concentration and the molar ratio (Fig. 5b); and molar ratio and temperature (Fig. 5c).

The response surface plot of conversion plotted against catalyst concentration and temperature (Fig. 5a) resulted in a conversion of > 70% between a temperature of 60–65 °C
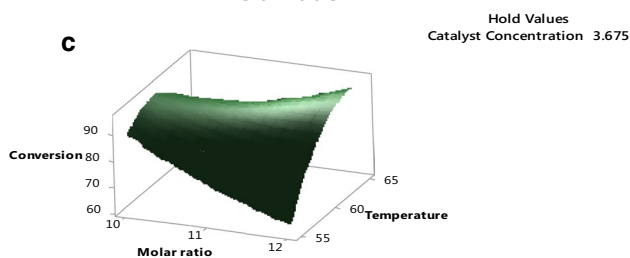

Fig. 5 a Response surface plot of conversion vs. temperature and catalyst concentration. **b** Response surface plot of conversion vs. molar ratio and catalyst concentration. **c** Response surface plot of conversion vs. temperature and molar ratio. **d** Contour plot of conversion vs.temperature and molar ratio. **e** Contour plot of conversion vs. molar ratio and catalyst concentration. **f** Contour plot of temperature vs. catalyst concentration

and catalyst concentration of 3.675–4.500 wt.%. At a molar ratio (methanol to oil) of 12:1 and catalyst concentration of 4.500 wt.%, the conversion reached > 96%. At molar ratio 12:1 (methanol to oil) and temperature of 65 °C, > 97% conversion was attained (Fig. 5c).

The contour plots for conversion were plotted against BC (Fig. 5d), AB (Fig. 5e) and AC (Fig. 5f). These plots were generated while holding one variable constant while the other two were varied over their entire range. The quadratic model for conversion is shown in the form of Eq. 4:
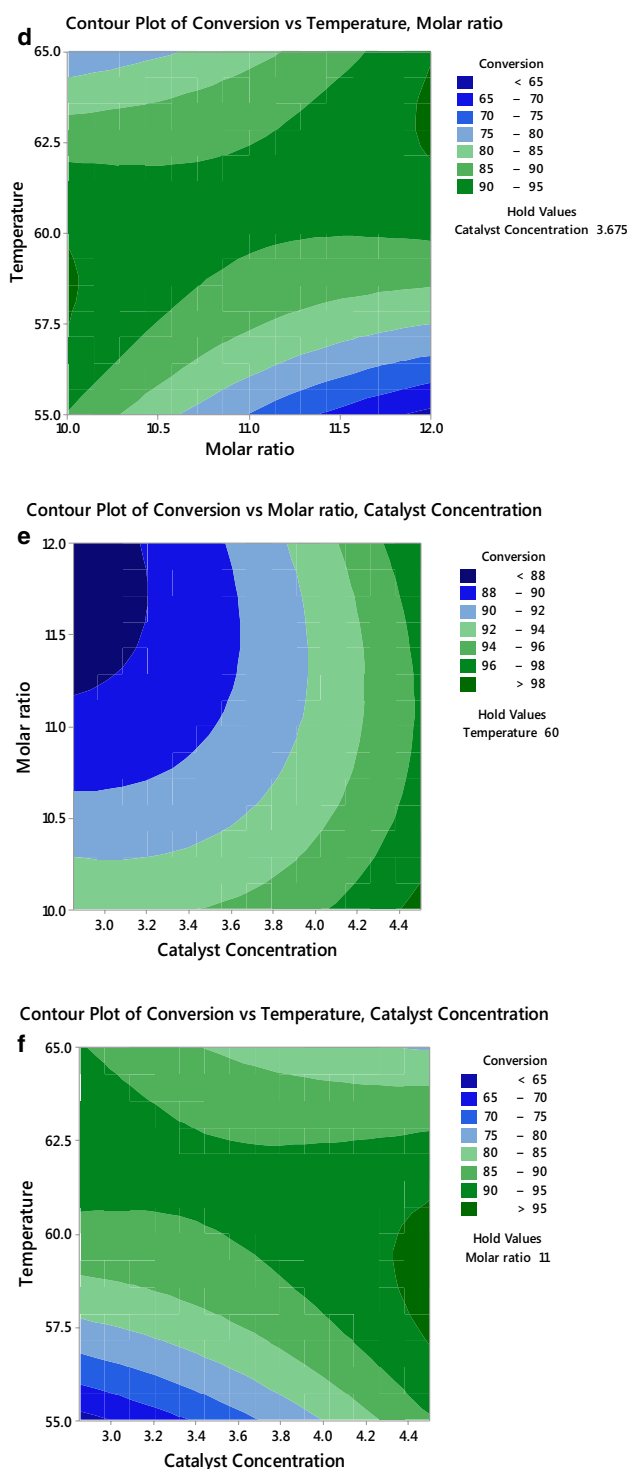
d Contour Plot of Conversion vs Temperature, Molar ratio

e Contour Plot of Conversion vs Molar ratio, Catalyst Concentration

f Contour Plot of Conversion vs Temperature, Catalyst Concentration

Fig. 5 (continued)

$$Y \text{ (conversion; \%)} = 96.41 + 3.9 \times A - 1.93 \times B + 4.31 \\ \times C + 1.54 \times A^2 - 1.12 \times B^2 - 0.95 \\ \times C^2 - 14.66 \times AB - 9.20 \times AC \\ - 11.15 \times BC - 1.12.$$
(4)

The coefficient of determination (R^2) value of 80.39% shows good fit of the model and suggested that a good degree of explanation exists for the observed variation in responses. This model was used to predict the value of responses for all the experimental runs (Table 2).

The regression coefficients, p value, and other parameters for the model terms are shown in Table 3. The highest coefficient was for the constant (96.41), which was statistically significant ($p < 0.05$). Among the model terms, only the squared term of reaction temperature (C^2), and the interaction terms AC (Catalyst × Temperature) and BC (Molar ratio × Temperature) were statistically significant.

The ANOVA done for the quadratic model are shown in Table 4. The F value and the p value for the regression model were 2.53 and 0.160 (insignificant), respectively. This indicates that the model could not explain the variability in response under different settings for the model terms. The F value of the linear, squared, and interaction effects was low and insignificant ($p > 0.05$). The model lack of fit was insignificant ($p = 0.794$) and thus it could be assumed that the model fits the data.

The ^{1}H NMR spectra of soybean oil after transesterification gave a conversion value of 97.61% (run number 2 & 12, Fig. 6). The characteristic peak of methoxy protons of biodiesel appears at 3.6 ppm. However, a conversion greater than 96.5% is desired for biodiesel to meet the international specification of EN 14,214:2003 [50]. A conversion of 96.61% was achieved in run number 15 with variables at same levels as in run number 2 & 12. The standard deviation and standard error of the three replicates (run number 2, 12, & 15) were 0.5773 and 0.3333, respectively. We conclude that a molar ratio of 11:1 (methanol to oil, catalyst concentration of 3.675 wt% (with respect to oil) at 60 °C in 2 h is the optimum condition for synthesis of biodiesel with acceptable quality.

Table 3 Regression coefficients and their significance levels

Coefficient	Value	SE	T value	p value
Constant	96.41	2.95	32.65	0.00
Linear				
A	3.87	1.81	2.14	0.085
B	−1.93	1.81	−1.07	0.334
C	4.31	1.81	2.39	0.063
Square				
A^2	−1.12	2.66	−0.42	0.692
B^2	−0.95	2.66	−0.36	0.737
C^2	−14.660	2.66	−5.48	0.003
Interaction				
AB	1.54	2.56	0.60	0.574
AC	−9.20	2.56	−3.60	0.016
BC	11.15	2.56	4.36	0.007

Table 4 Analysis of variance (ANOVA) for the quadratic model

Source	DF	AdjSS	AdjMS	F value	p value	Remarks
Regression	9	1703.23	189.248	2.53	0.160	Insignificant
Linear	3	298.60	99.533	1.33	0.363	
Square	3	559.14	186.380	2.49	0.175	
Interaction	3	845.49	281.830	3.76	0.094	
Error	5	374.49	74.897			
Lack of fit	3	130.81	43.605	0.36	0.794	
Pure error	2	243.67	121.836			
Total	14	2077.71				
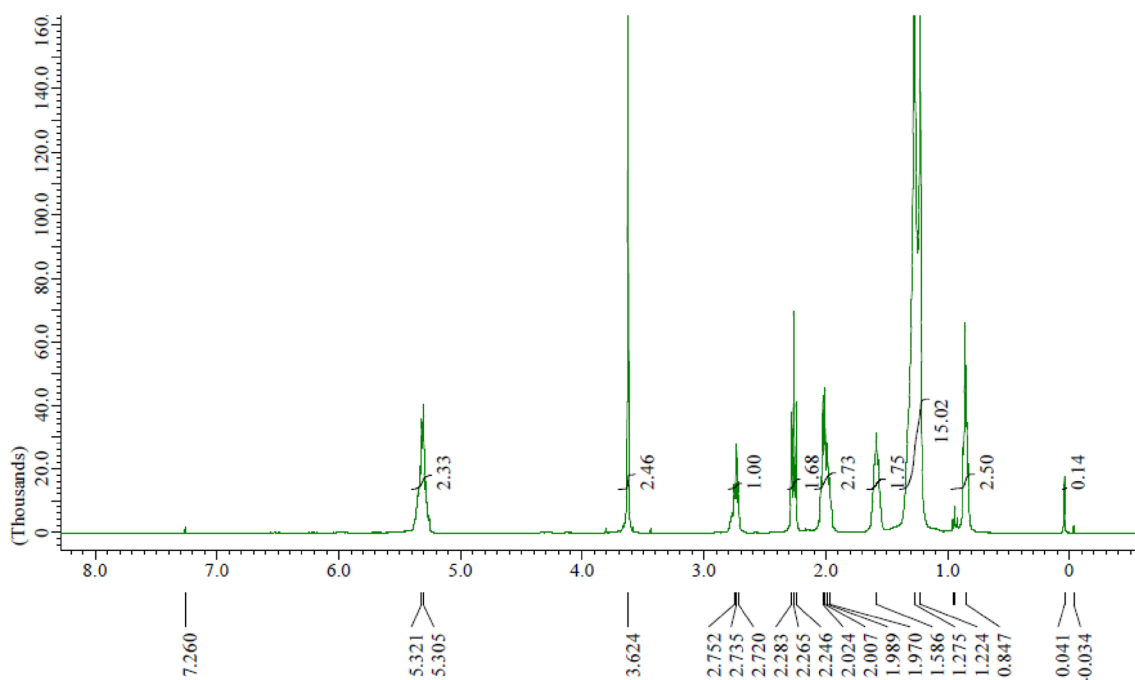
Fig. 6 ^{1}H NMR spectra of transesterified soybean oil

Nanomaterials have been shown to exhibit high adsorption capacity as compared to conventional adsorbents [51]. In the process of catalysis, the mechanism involved is adsorption. With a small particle size, a greater number of active sites would be available for transesterification. Hence, the prepared nanocatalyst can be assumed to offer a better catalytic activity. Nanomaterials also offer a lower secondary pollution issues and a better simplicity in its usage [52].

Leaching studies were not conducted in the present study. However, Badnore et al. [13] reported that leaching of nano-CaO was negligible during synthesis of biodiesel by ultrasound mode of reaction. In terms of material balance, only 0.313 mg of catalyst was reported to be lost after decantation. The reuse of nano-CaO with a loss of 20% efficiency in the third consecutive run was reported by Banković–Ilić et al. [16]. Precursors and carriers can be used to further enhance the catalytic activity and reusability of the nano-CaO as catalyst. 80% of the total cost of biodiesel production is attributed to the feedstock [53]. The cost of nano-CaO will not be significantly higher than the other routes of preparation of CaO. The reusability of the heterogeneous catalyst (CaO and nano-CaO) will make the overall cost of catalyst less significant compared to other cost attributes (feedstock, energy consumption, manpower, etc.).

This study indicates environmental as well as economic significance for synthesis of biodiesel at moderate reaction conditions that meets international specifications. Most prior studies reported that a high reaction temperature and long reaction time were needed for similar conversion of biodiesel. Sharma et al. [54] have reported a conversion of biodiesel from *Pongamia pinnata* oil at a reaction temperature of 65 ± 0.5 °C for 2.5 h using 2.5 wt% catalyst and 8:1 (alcohol to oil) molar ratio. Although a higher molar ratio was used in our study, the excess methanol can be separated from the

product and reused for further reaction. Similarly, the catalyst (CaO) is widely available through waste products from any material composed of calcium carbonate such as chicken eggshells. High reaction temperature and longer reaction time contribute significant cost to the commercial production of biodiesel. Thus, synthesis of biodiesel using a moderate reaction temperature and reaction time should make commercial production of biodiesel more economically viable.

Conclusion

The transesterification of soybean oil using a nano-CaO catalyst synthesized via sol–gel method was optimized through response surface methodology. A high conversion of 97.61% was obtained at a catalyst loading of 3.675 wt% (with respect to oil), molar ratio of 11:1 (methanol to oil) at 60 °C for 2 h. The synthesized calcium oxide nanocatalyst exhibited a high conversion efficiency of soybean oil to biodiesel under moderate reaction conditions. The catalyst had a higher conversion rate compared to other CaO-based catalysts. The higher conversion can be attributed to the higher surface area of the nano-CaO compared to the larger sized CaO.

References

1. Islam, A., Taufiq-Yap, Y.H., Chan, E.S., Moniruzzaman, M., Islam, S., Nabi, M.N.: Advances in solid-catalytic and non-catalytic technologies for biodiesel production. Energy Convers. Manage. **88**, 1200–1218 (2014)

2. Nas, B., Berktay, A.: Energy potential of biodiesel generated from waste cooking oil: an environmental approach. Energy Sources B Econ Plan Policy. **2**, 63–71 (2007)

3. Arzamendi, G., Campo, I., Arguinarena, E., Sanchez, M., Montes, M., Gandia, L.M.: Synthesis of biodiesel with heterogeneous NaOH/alumina catalysts: comparison with homogeneous NaOH. Chem. Eng. J. **134**, 123–130 (2007)

4. Reyero, I., Arzamendi, G., Gandia, L.M.: Heterogeneization of the biodiesel synthesis catalysis: CaO and novel calcium compounds as transesterification catalysts. Chem. Eng. Res. Des. **92**, 1519–1530 (2014)

5. Ilic, I.B.B., Miladinovic, M.R., Stamenkovic, O.S., Veljkovic, V.B.: Application of nano CaO-based catalysts in biodiesel synthesis. Renew. Sust. Energy Rev. **72**, 746–760 (2017)

6. Shi, M., Zhang, P., Fan, M., Jiang, P., Dong, Y.: Influence of crystal of Fe_2O_3 in magnetism and activity of nanoparticle CaO@Fe_2O_3 for biodiesel production. Fuel **197**, 343–347 (2017)

7. Rochat, W., Phewphong, S., Thangthong, A., Moonsin, P., Yoosuk, B., Kaewpuang, T., Promarak, V.: Catalytic performance enhancement of CaO by hydration-dehydration process for biodiesel production at room temperature. Energy Convers. Manage. **165**, 1–7 (2018)

8. Todorovic, Z.B., Troter, D.Z., Stojanovic, D.R.D., Velickovic, A.V., Avramovic, J.M., Stamenkovic, O.S., Veselinovic, L.M., Veljkovic, V.B.: Optimization of CaO-catalyzed sunflower oil methanolysis with crude biodiesel as a cosolvent. Fuel **237**, 903–910 (2019)

9. Degirmenbasi, N., Coskun, S., Boz, N., Kalyon, D.M.: Biodiesel synthesis from canola oil via heterogeneous catalysis using funtionalized CaO nanoparticles. Fuel **153**, 620–627 (2015)

10. Seffati, K., Honarvar, B., Esmaeili, H., Esfandiari, N.: Enhanced biodiesel production from chicken fat using CaO/$CuFe_2O_4$ nanocatalyst and its combination with diesel to improve fuel properties. Fuel **235**, 1238–1244 (2019)

11. Hu, S., Guan, Y., Wang, Y., Han, H.: Nano-magnetic catalyst KF/CaO-Fe_3O_4 for biodiesel production. Appl. Energy **88**, 2685–2690 (2011)

12. Salimi, Z., Hosseini, S.A.: Study and optimization of conditions of biodiesel production from edible oils using ZnO/$BiFeO_3$ nano magnetic catalyst. Fuel **239**, 1204–1212 (2019)

13. Badnore, A.U., Jadhav, N.L., Pinjari, D.V., Pandit, A.B.: Efficacy of newly developed nano-crystalline calcium oxide for biodiesel production. Chem. Eng. Process. **133**, 312–319 (2018)

14. Hebbar, H.R.H., Math, M.C., Yatish, K.V.: Optimization and kinetic study of CaO nano-particles catalysed biodiesel production from Bombax coiba oil. Energy **143**, 25–34 (2018)

15. Hsiao, M.C., Lin, C.C., Chang, Y.H.: Microwave irradiation-assisted transesterification of soybean oil to biodiesel catalysed by nanopowder calcium oxide. Fuel **90**, 1963–1967 (2011)

16. Banković-Ilić, I.B., Miladinovic, M.R., Stamenkovic, O.S., Veljkovic, V.B.: Application of nano CaO-based catalysts in biodiesel synthesis. Renew Sust Energ Rev **72**, 746–760 (2017)

17. Teo, S.H., Islam, A., Chan, E.S., Choong, S.Y.T., Awual, M.R.: Efficient biodiesel production from *Jatropha curcas* using $CaSO_4$/Fe_2O_3-SiO_2 core-shell magnetic nanoparticles. J. Clean. Prod. **208**, 816–826 (2019)

18. Awual, M.R., Miyazaki, Y., Taguchi, T., Shiwaku, H., Yaita, T.: Encapsulation of cesium from contaminated water with highly selective facial-organic inorganic mesoporous hybrid adsorbent. Chem. Eng. J. **291**, 128–137 (2016)

19. Awual, M.R.: Solid phase sensitive palladium (II) ions detection and recovery using ligand based effective conjugate nanomaterials. Chem. Eng. J. **300**, 264–272 (2016)

20. Awual, M.R., Hasan, M.M., Khaleque, M.A., Sheikh, M.C.: Treatment of copper (II) containing wastewater by a newly developed ligand based facial conjugate materials. Chem. Eng. J. **288**, 368–376 (2016)

21. Awual, M.R., Rahman, I.M.M., Yaita, T., Khaleque, M.A., Ferdows, M.: pH dependant Cu(II) and Pd(II) ions detection and removal from aqueous media by an efficient mesoporous adsorbent. Chem. Eng. J. **236**, 100–109 (2014)

22. Shahat, A., Awual, M.R., Naushad, M.: Functional ligand anchored nanomaterial based facial adsorption for cobalt (II) detection and removal from water samples. Chem. Eng. J. **271**, 155–163 (2015)

23. Awual, M.R., Alharthi, N.H., Hasan, M.M., Karim, M.R., Khaleque, M.A.: Inorganic-organic- based nano-conjugate

adsorption for selective palladium (II) detection, separation and recovery. Chem. Eng. J. **324**, 130–139 (2017)

24. Awual, M.R., Alharthi, N.H., Okamoto, Y., Karim, M.R., Sheikh, M.C.: Inorganic-organic- based nano-conjugate adsorption for selective palladium (II) detection, separation and recovery. Chem. Eng. J. **320**, 427–435 (2017)

25. Awual, M.R., Hasan, M.M., Eldesoky, G.E., Khaleque, M.A., Naushad, M.: Facile mercury detection and removal from aqueous media involving ligand impregnated conjugate nanomaterials. Chem. Eng. J. **290**, 243–251 (2016)

26. Awual, M.R., Hasan, M.M., Shahat, A., Naushad, M., Yaita, T.: Investigation of ligand immobilized nano-composite adsorbent for efficient cerium (III) detection and recovery. Chem. Eng. J. **265**, 210–218 (2015)

27. Awual, M.R., Yaita, T., Taguchi, T., Shiwaku, H., Okamoto, Y.: Selective cesium removal from radioactive liquid waste by crown ether immobilized new class conjugate adsorbent. J. Hazard. Mater. **278**, 227–235 (2014)

28. Awual, M.R., Suzuki, S., Taguchi, T., Shiwaku, H., Yaita, T.: Radioactive cesium removal from nuclear wastewater by novel inorganic and conjugate adsorbents. Chem. Eng. J. **242**, 127–135 (2014)

29. Awual, M.R., Ismael, M., Yaita, T., Safty, S.A.E., Suzuki, S.: Trace copper (II) ions detection and removal from water using novel ligand modified composite adsorbent. Chem. Eng. J. **222**, 67–76 (2013)

30. Awual, M.R., Yaita, T., Safty, S.A.E., Shiwaku, H., Okamoto, Y.: Copper (II) ions capturing from water using ligand modified a new type mesoporous adsorbent. Chem. Eng. J. **221**, 322–330 (2013)

31. Awual, M.R.: New type mesoporous conjugate material for selective optical copper (II) ions monitoring and removal from polluted waters. Chem. Eng. J. **307**, 85–94 (2017)

32. Awual, M.R.: Novel nanocomposite materials for efficient and selective mercury ions capturing from wastewaters. Chem. Eng. J. **307**, 456–465 (2017)

33. Awual, M.R.: Ring sized dependant crown ether based mesoporous adsorbent for high cesium adsorption from wastewater. Chem. Eng. J. **303**, 539–546 (2016)

34. Awual, M.R.: Assessing of lead (III) capturing from contaminated wastewater using ligand doped conjugate adsorbent. Chem. Eng. J. **289**, 65–73 (2016)

35. Awual, M.R.: A novel facial composite adsorbent for enhanced copper (II) detection and removal from wastewater. Chem. Eng. J. **266**, 368–375 (2015)

36. Shahat, A., Awual, M.R., Khaleque, M.A., Alam, M.Z., Naushad, M., Chowdhury, A.M.S.: Large-pore diameter nano-adsorbent and its application for rapid lead(II) detection and removal from aqueous media. Chem. Eng. J. **273**, 286–295 (2015)

37. Awual, M.R., Khraisheh, M., Alharthi, N.H., Luqman, M., Khaleque, M.A.: Efficient detection and adsorption of cadmium (II) ions using innovative nano-composite materials. Chem. Eng. J. **266**, 118–127 (2018)

38. Tahvildari, K., Anaraki, Y.N., Fazaei, R., Mirpanji, S., Delrish, E.: The study of CaO and MgO heterogenic nano-catalyst coupling on transesterification reaction efficacy in the production of biodiesel from recycled cooking oil. J. Environ. Health Sci. **13**(73), 1–9 (2015)

39. Knothe, G.: Analyzing Biodiesel: standard and other methods. JAOCS. **83**, 823–833 (2006)

40. Singh, V., Belova, L., Singh, B., Sharma, Y.C.: Biodiesel production using a novel heterogeneous catalyst, magnesium zirconate ($Mg_2Zr_5O_{12}$): process optimization through response surface methodology (RSM). Energy Convers. Manage. **174**, 198–207 (2018)

41. Kumar, D., Singh, B.: $BaZrO_3$ and Cs- $BaZrO_3$ catalyzed transesterification of *Millettia pinnata* oil and optimization of reaction variables by response surface Box-Behnken design. Renew. Energy **133**, 411–421 (2019)

42. Fan, M., Liu, Y., Zhang, P., Jiang, P.: Blocky shapes Ca–Mg mixed oxides as a water resistant catalyst for effective synthesis of biodiesel by transesterification. Fuel Process. Technol. **149**, 163–168 (2016)

43. Awual, M.R., Yaita, T., Shiwaku, H.: Design a novel optical adsorbent for simultaneous ultra-trace cerium (III) detection, sorption and recovery. Chem. Eng. J. **228**, 327–335 (2013)

44. Awual, M.R., Yaita, T., Shiwaku, H., Suzuki, S.: A sensitive ligand embedded nano-conjugate adsorbent for effective cobalt (II) ions capturing from contaminated water. Chem. Eng. J. **276**, 1–10 (2015)

45. Kouzu, M., Hidaka, J.: Transesterification of vegetable oil into biodiesel catalyzed by CaO: a review. Fuel **93**, 1–12 (2012)

46. Pandit, P.R., Fulekar, M.H.: Biodiesel production from micfroalgal biomass using CaO catalyst synthesized from natural waste material. Renew. Energy **136**, 837–845 (2019)

47. Awual, M.R., Hasan, M.M., Rahman, M.M., Asiri, A.M.: Novel composite material for selective copper (II) detection and removal from aqueous media. J. Mol. Liq. **283**, 772–780 (2019)

48. Awual, M.R., Hasan, M.M., Znad, H.: Organic-inorganic based nano-conjugate adsorption for selective palladium (II) detection, separation and recovery. Chem. Eng. J. **259**, 611–619 (2015)

49. Awual, M.R.: Innovative composite material for efficient and highly selective Pb(II) ion capturing from wastewater. J. Mol. Liq. **284**, 502–510 (2019)

50. Kumar, D., Singh, B.: $BaZrO_3$ and Cs-$BaZrO_3$ catalysed transesterification of *Millettia Pinnata* oil and optimisation of reaction variables by response surface Box-Behnken design. Renew. Energy **133**, 411–421 (2019)

51. Awual, M.R., Islam, A., Hasan, M.M., Rahman, M.M., Asiri, A.M., Khaleque, M.A., Sheikh, M.C.: Introducing an alternative conjugated material for enhanced lead (II) capturing from wastewater. J. Clean. Prod. **224**, 920–929 (2019)

52. Awual, M.R., Eldesoky, G.E., Yaita, T., Naushad, M., Shiwaku, H., AlOthman, Z.A., Suzuki, S.: Schiff based ligand containing nano-composite adsorbent for optical copper (II) ions removal from aqueous solutions. Chem. Eng. J. **279**, 639–647 (2015)

53. Sharma, Y.C., Singh, B., Upadhyay, S.N.: Advancements in development and characterization of biodiesel: a review. Fuel **872**, 2355–2373 (2008)

54. Sharma, Y.C., Singh, B., Korstad, J.: Application of an efficient nonconventional heterogeneous catalyst for biodiesel synthesis from *Pongamia pinnata* oil. Energy Fuel **24**, 3223–3231 (2010)

Affiliations

Priyanka Bharti[1] · Bhaskar Singh[1] · R. K. Dey[2]

[1]   Department of Environmental Sciences, Central University of Jharkhand, Brambe, Ranchi 835205, India

[2]   Department of Chemistry, Central University of Jharkhand, Brambe, Ranchi 835205, India